A high-voltage transmission-line pulse transformer with very low droop

P. N. Graneau, J. O. Rossi, M. P. Brown, and P. W. Smith
Department of Engineering Science, University of Oxford, Oxford OX1 3PJ, United Kingdom

(Received 23 January 1996; accepted for publication 1 April 1996)

The design, construction, and operational characteristics of a 200 kV transmission line pulse transformer is described. The transformer is wound using a new winding method that enhances the isolation of the output of the transformer from the input. As a result, pulse droop is substantially reduced, minimizing pulse distortion in the transformer. The ways in which both pulse rise time and droop can be further improved are investigated using a simple model for the transformer. The frequency response performance of the transformer is also described and modeled. As a result, it is shown that this type of transformer has the potential to be used as a high-frequency, continuously excited power transformer. © *1996 American Institute of Physics.* [S0034-6748(96)03307-2]

I. INTRODUCTION

There is increasing interest in the use of transmission line pulse transformers for a variety of applications, where the peak pulse power is of the order of a few hundred MW or less and the pulse amplitudes are in the region of a few hundred kV. Factors such as the constructional simplicity of the devices and low cost often influence the designer of pulsed power supplies to use these devices, particularly if there is a requirement for repetitive operation of the supply. One significant problem that has limited more widespread use of these devices has been a lack of a proper understanding of the way in which these devices work and adequate circuit models from which detailed design calculations can be made. Two articles that address the modeling issue and also review the wide variety of different types of devices that have been made have recently been written.[1,2] From this work it would appear that the potential performance capabilities and range of applications for which this class of transformer can be used are more significant than has previously been realized.

The transformer described in this article was built as a test device to investigate, in particular, rise time, gain, and pulse droop capabilities of a high voltage transmission line transformer capable of output voltages up to 200 kV when operated in air. Rise time and pulse droop have always been problem issues for designers of conventional magnetically cored pulse transformer, particularly in the case of high voltage transformers with large turn ratios. In such devices, leakage inductance in the primary winding and stray capacitance in the secondary can severely limit output rise time. If the number of turns on the transformer is restricted in order to reduce the stray capacitance, the primary inductance is reduced and consequently pulse droop becomes worse.[3] The transformer described in this article features a rise time/pulse droop capability that would be very difficult to achieve in a conventional pulse transformer with the same operating voltage and voltage gain. Furthermore, performance measurements on the transformer and their analysis indicate fairly simple ways in which the rise time and pulse droop capabilities could be further extended in this type of device.

The low pulse droop exhibited by the transformer should be of considerable interest to the designers of linear accelerators that use high power klystrons to accelerate the beam. Pulse droops of less than 1% over pulse lengths up to 1 μs are often specified for the pulsed power source used to drive the klystrons in order to minimize power and phase variations between the accelerating cavities.[4]

II. CONSTRUCTION

The basic construction of the transformer can be seen by reference to the circuit diagram shown in Fig. 1 and the photograph of the transformer given in Fig. 2. The transformer was constructed using ten lengths of URM 67 coaxial cable, each of which is 110 m long. This cable has an impedance of 50 Ω, an outside diameter of 10.3 mm, and a maximum dc operating voltage of 40 kV. The basic construction of the transformer exploits the benefits of mutually coupling the cable windings, at each stage of the transformer, to enhance the inductive isolation of the output of the transformer from the input.[2] This winding technique also ensures that the inductive isolation to ground, from the output of the transformer to the input, increases from the bottom stage upwards and has the added benefit that the potential difference between the top and bottom stage of the transformer is uniformly divided between each of the ten stages of the transformer. The transformer was wound through nine sets of ferrite cores, one set for all but the bottom stage of the transformer. Each set of cores comprised 18 rectangular cores made from four clamped ''I'' shaped cores and were mounted radially on the circumference of a large PVC tube 40 mm in diameter. The cores were made of 3C8 (A16)[5] MnZn ferrite that is commonly used to make power transformers for switched mode power supplies and the magnetic area of the cores was 625 mm^2. The magnetic length of the cores was reduced in the top stages of the transformer to minimize its weight and size. This is possible as the volume, occupied by the windings, reduces from the bottom to the top stages of the transformer. Each stage of the transformer, with its corresponding set of cores, was separated from its neighbors by an annular ring of perspex that was glued to the PVC tube to minimize the chance of electrical breakdown between the stages, and the whole winding/core structure was supported with threaded lengths of nylon rod that were bolted at each stage. The overall height of the transformer was 1.3 m.

 0034-6748/96/67(7)/2630/6/$10.00

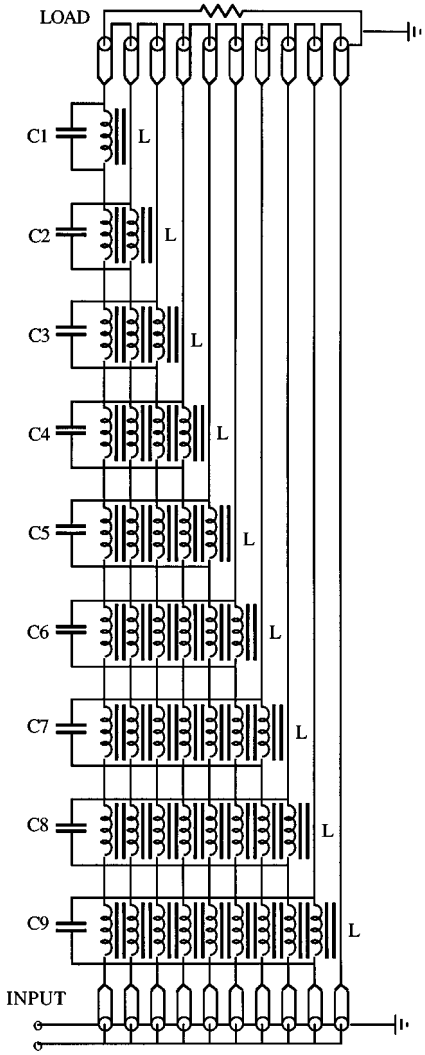

FIG. 1. Equivalent circuit of the ten-stage transformer.

The transformer was wound by taking nine of the cables and winding them, in a spiral fashion, seven times through the lowest set of ferrite cores on the PVC tube. The first stage of the transformer was made by passing the tenth cable through a hole in the bottom of the tube and making it the bottom cable in the series connection of the output ends of the cables shown in Fig. 1. The next stage of the transformer was made by winding eight of the remaining nine cables again seven times through the next set of 18 cores adjacent to the bottom set. The ninth cable was then passed into the tube and connected in series with the output of the first stage of the transformer. This process was repeated at each stage by winding all but one of the remaining cables on separate sets of cores and connecting the unwound cable in series with the output of the preceding stage. In this way the top stage comprises just one cable that, when connected in series with the penultimate cable in the stack, completes the construction and winding of the transformer. The series connection of the output ends of the cables was made vertically, up the center of the PVC tube on which the windings were mounted. As only one of the cables is wound through all nine sets of cores, there is the problem of storing quite large lengths of cable. This was done by winding the cables, prior to winding the transformer, on a second PVC tube that is shown to the right of the transformer in Fig. 2. Clearly, the longest winding on this tube results from the bottom cable of the transformer with successive cables in the transformer occupying a decreasing amount of space on the second tube as their winding length in the transformer stack increases.

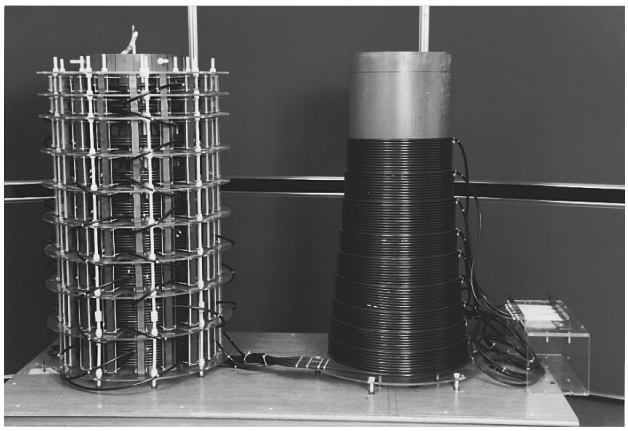

FIG. 2. Photograph of the complete transformer assembly.

Load resistors were connected to the output of the transformer by running the load and its connecting conductors down the center of the transformer in parallel with the insulating rod used to support the vertical, series connection of the output of the cables. A low inductance connection to the input of the transformer was made by stripping back the braiding of the cables by 100 mm and soldering the inner conductors of the cables to a length of brass sheet. The braiding of each of the cables was then connected to a second brass sheet that was run under the set of inner conductors and insulated from them by sheet of perspex. The arrangement can be seen on the far right hand side of the photograph in Fig. 2.

The transformer was operated in air so that modifications to the transformer structure and electrical measurements on the transformer could conveniently be made. This meant that the maximum operating voltage of the transformer was restricted to 200 kV due to electrical breakdown problems within the transformer structure when operated above this voltage. There is no reason why the transformer could not be operated under oil when it should be possible to approach an operating potential close to ten times the maximum operating potential of an individual cable. It should be noted, however, that internal breakdown of individual cables, due to corona discharges between the cable conductors and the insulating dielectric, will reduce this operating potential to a figure below the maximum dc operating potential quoted earlier.[6] This problem is exacerbated if such transformers are run at high repetition rates. Performance data from the manufacturer of URM 67[7] cable recommends a maximum pulse operating voltage of 13 kV although experience in operating this and other transmission line transformers[8] would suggest that this figure is rather conservative and that the cable can be safely run at around twice this voltage.

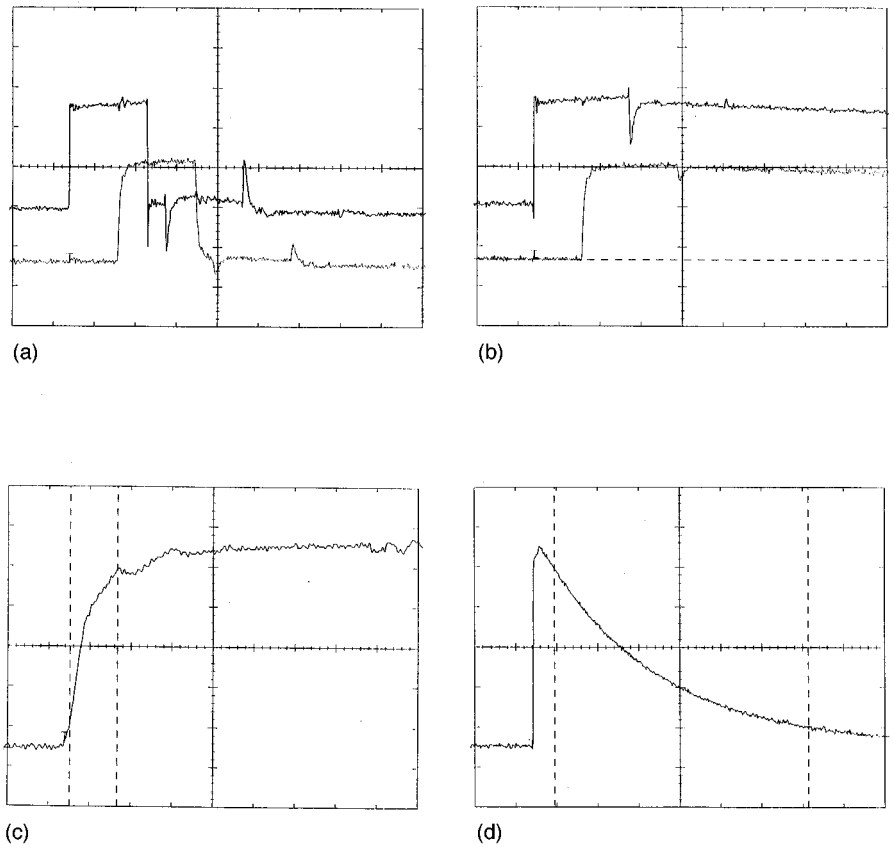

FIG. 3. Low voltage input and output wave forms from the transformer. Arbitrary vertical scale (a) Input and output wave forms 500 ns/horizontal division—1 μs input pulse. (b) Input and output wave forms 500 ns/horizontal division—100 μs input pulse. (c) Output wave form 50 ns/horizontal division. 10%–90% rise marked 57.5 ns. (d) Output wave form 10 μs/horizontal division. 90%–10% fall marked 61.9 μs.

III. PERFORMANCE

The operating characteristics of the transformer as a pulse transformer were investigated both at low voltage and at the maximum voltage that the transformer would withstand without breakdown (200 kV). At low voltage a pulse generator, with pulse rise and fall times $\leqslant$6 ns (Philips PM5715), was connected to the input of the transformer via a 47 Ω resistor to ensure that the 50 Ω output impedance of the generator was matched. Since the input impedance of the transformer is just 5 Ω, care was taken to minimize the stray inductance of the connection to prevent an increase in pulse rise time. The output of the transformer was connected to a carbon composite 500 Ω load resistor as described in Sec. II. Observation of both the input and output wave forms was made using a Tektronix 2440 oscilloscope. The results of these tests are shown in Fig. 3.

In Fig. 3(a), input and output wave forms are shown for 1 μs input pulse, the output pulse being the lower of the two wave forms. The output pulse wave form, attenuated by a factor of 10 compared to the input pulse, shows negligible droop and some increase in rise time due to the stray capacitance in the spiral cable windings of the transformer. This capacitance causes a mismatch to the output impedance of the transformer at the start of the pulse and consequently a negative spike is propagated back to the input of the transformer. This spike can clearly be seen on the input wave form after the input pulse has terminated. The amplitudes of the input and the attenuated output pulses are virtually the same, when the transformer is operated under matched conditions, indicating that the gain of the transformer is very close the theoretical gain of 10. The leading edge of the output wave form is expanded and displayed in Fig. 3(c), where it can be seen that the 10%–90% rise time is of the order of 65 ns if the spurious ''bump'' on the rising edge of the wave form is disregarded. A longer, 100 μs pulse was also injected into the transformer to investigate its ability to maintain ''flat top'' performance over relatively long time scales. In Fig. 3(b), very little droop is evident in the output pulse over a duration of several μs, and in Fig. 3(d) the 90%–10% droop, on a much longer time scale, can be seen to be 61.9 μs.

At high voltages, the low input impedance of the pulse transformer makes it difficult to produce a pulse of sufficient quality to adequately test the performance capabilities of the transformer. This problem was solved by building a 1 μs pulse forming line using the paralleled lengths of URM 67 coaxial cable, which gives a perfect match to the input impedance of the transformer. To minimize pulse distortion, a pressurized rail spark gap was used to switch the pulse forming line into the transformer through a carefully engineered, low inductance feed. To inject a pulse of 20 kV into the transformer, the line was charged to 40 kV and the results of this test are shown in Fig. 4. The output voltage wave form again has a slight increase in rise time with negligible droop

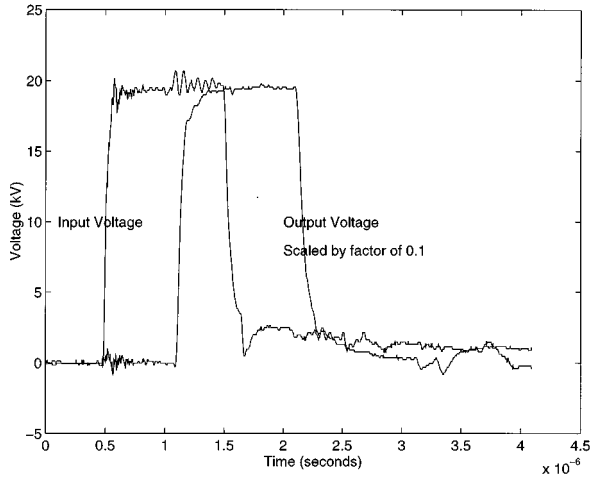

FIG. 4. Input and output wave forms of the transformer at full operating voltage.

and has an amplitude that is very close to the theoretical maximum of 200 kV. Clearly, the performance of this transformer as a high voltage pulse transformer is exceptional in comparison to the level of performance that is to be expected from conventional magnetically core devices.

Both the observed rise time and droop can accurately be accounted for using the reflection model for this type of transformer discussed elsewhere.[2] Equivalent circuits for both the output and input circuits of the transformer can be found by this method, and the resulting circuits are presented in Fig. 5. In the output circuit, it has been assumed that the inductance at each stage of the winding is the same despite the fact that the magnetic length of the cores in the top two and bottom two stages of the transformer are slightly smaller and larger, respectively, than the length of the remaining middle stages. The variation in the measured inductance at

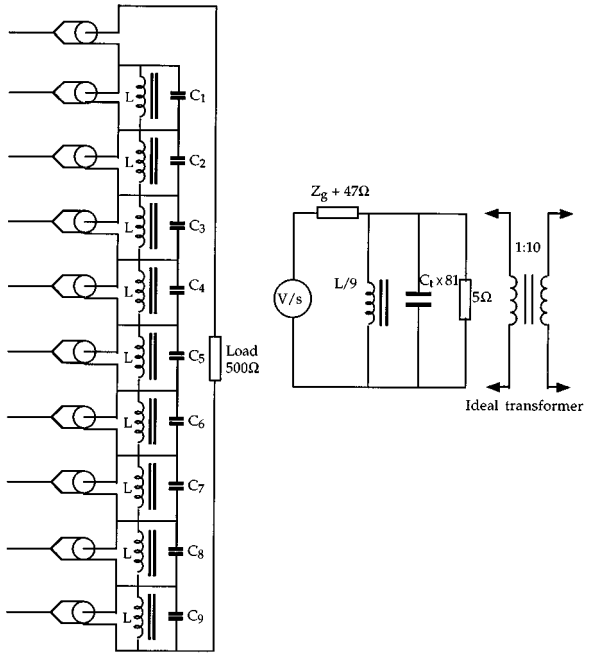

FIG. 5. Equivalent circuits of the output and input of the transformer.

the different stages ranged from 1.9 mH (top) to 1.26 mH (bottom). The effect of this variation was minimized by estimating, from the measured values, an average value of the inductance L per stage of 1.35 mH that is used in the performance calculations. An estimate of the stray capacitance across the spiral windings, at each stage of the transformer, was obtained by isolating the top stage of the transformer and measuring its self-resonant frequency. This was done by connecting a signal generator to both ends of the outer conductor of the cable that forms the top winding. From the measured inductance of this winding and the self-resonant frequency, it was possible to calculate a value for its stray capacitance (C_1) of 130 pF. The stray capacitance of the remaining windings (C_2 to C_9) was estimated by multiplying this value by the number of cables in a given winding and adding to the resulting figure an additional estimated capacitance to allow for stray capacitance between windings. The total stray secondary capacitance across the output of the transformer C_t was then calculated as the series combination of the stray capacitances of all nine windings, giving a value of 70 pF. Reflecting both the total stage inductance and total stray capacitance to the input circuit gives a very simple circuit (Fig. 5), from which approximate values of both rise time and fall time can be calculated and compared to the experimental values. This analysis leads to the following expressions:

$$v_0(t) = V\,\frac{5}{Z+5}\,\exp\left(-\frac{45Zt}{L(Z+5)}\right)\ \text{(fall time)}, \tag{1}$$

$$v_0(t) = V\,\frac{5}{Z+5}\left[1-\exp\left(-\frac{(Z+5)t}{405ZC}\right)\right]\ \text{(rise time)}, \tag{2}$$

where Z is the sum of the output impedance of the generator and the value of the matching resistor (97 Ω), L is the average stage inductance, and C_t is the total stray capacitance. Using the values of L and C_t given above gives calculated values for the 10 to 90% rise and fall times of 59 ns and 69 μs respectively. These times are in close agreement with the observed values.

IV. FREQUENCY RESPONSE

As a further evaluation of the performance capabilities of the transformer, the frequency dependence of the voltage gain of the transformer was measured from very low frequencies to 5 MHz. These measurements were again taken under matched conditions (i.e., a sinusoidal signal generator was matched to the input of the transformer with a series 47 Ω resistor and the output was connected to a 500 Ω load) and the results, which are normalized to a maximum gain of 10, are shown in Fig. 6. The resulting frequency response curve is quite similar to that which is obtained for conventional transformers,[9] with the exception that the frequency response curve is shifted at both the low and high frequency cutoff points to higher frequencies. As the frequency is increased, the transformer reaches full gain at a frequency of approximately 1 kHz and it maintains full gain to a frequency of 300 kHz, at which point the gain starts to fall and is modulated by what appears to be an oscillatory response characteristic.

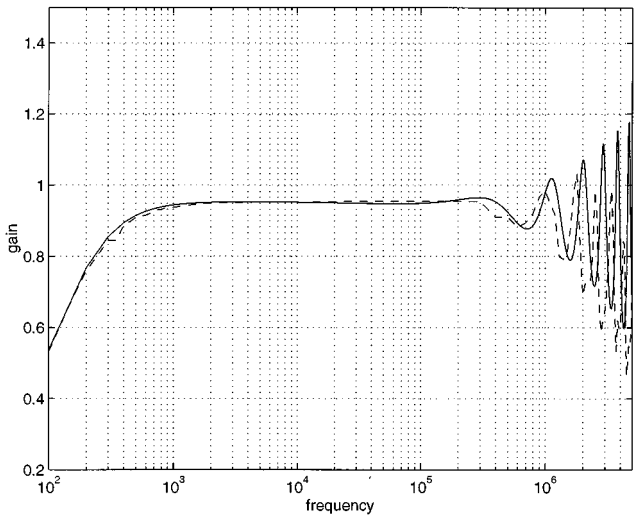

FIG. 6. Calculated (solid line) and observed (broken line) frequency response curves for the transformer. The maximum gain for both curves is normalized.

The shape of the gain versus frequency response curve can be quite accurately accounted for using the simple equivalent circuit of the output side of the transmission line transformer and load given in Fig. 7. In this circuit the transformer is represented as a single 500 Ω transmission line that is terminated by a matched 500 Ω load in parallel with the total stray capacitance of the spiral windings and an inductance L_t equal to the sum of the stage inductances as estimated above. The effect of the dc resistance of the lines is included in the circuit by adding a resistor R_{dc} in series with the input whose value (12 Ω) is equal to ten times the measured dc resistance of the inner and outer conductors of an individual, 110 m length, of line.

Starting from the standard matrix relationship[10] that connects the input (i) and output (T) currents and voltages of a length of transmission line with length l and propagation constant γ:

$$\begin{pmatrix} V_i \\ I_i \end{pmatrix} = \begin{pmatrix} \cosh\ \gamma l & Z_0 \sinh\ \gamma l \\ Z_0^{-1} \sinh\ \gamma l & \cosh\ \gamma l \end{pmatrix} \begin{pmatrix} V_T \\ I_T \end{pmatrix}, \tag{3}$$

the voltage transfer function of the equivalent circuit of the transformer and load as a function of complex frequency can be derived. Referring to Fig. 7, the voltage transfer function from the input of the line (to the right of R_{dc}) to the load is given by

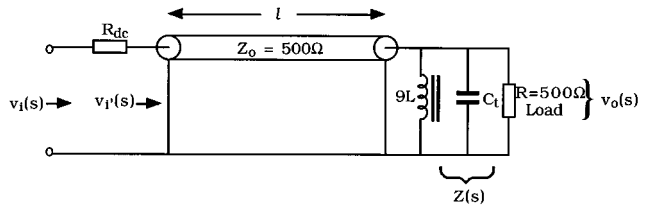

FIG. 7. Equivalent circuit of the transformer for determining its frequency response.

$$\frac{v_o(s)}{v_i'(s)} = T'(s) = \frac{Z(s)}{Z_0 \sinh\ \gamma l + Z(s) \cosh\ \gamma l}, \tag{4}$$

where $Z(s)$ is the impedance of the parallel combination of the total stray capacitance, the sum of the stage inductances, and the resistance of the load. If the input current to the line is $i_i(s)$, then the complete voltage transfer function from the input of the transformer (to the left of R_{dc}) to the output is given by

$$\frac{v_o(s)}{v_i(s)} = T(s) = \frac{1}{[R_{\mathrm{dc}} i_i(s)/v_o(s)] + [1/T'(s)]}. \tag{5}$$

From Eq. (3), the input current $i_i(s)$ can be eliminated using the derived relationship:

$$\frac{i_i(s)}{v_o(s)} = \frac{\sinh\ \gamma l}{Z_0} + \frac{\cosh\ \gamma l}{Z(s)}. \tag{6}$$

Due to the skin effect, the propagation constant of the cables γ will depend through the attenuation constant α and phase constant β on frequency. The frequency dependence of α was calculated[11] from the physical dimensions of URM 67 cable to take the form:

$$\alpha = 4.971 \times 10^{-7} \sqrt{f}\ \ \mathrm{m}^{-1},$$

where f is the frequency. A value for the phase constant β was derived using the inductance and capacitance per metre of the cable. The magnitude of the transfer function $|T(j\omega)|$ [Eq. (5)] was plotted from Eqs. (4)–(6) using MATLAB[12] in order to obtain a theoretical, normalized, frequency response curve for the transformer (Fig. 6) based on the equivalent circuit of Fig. 7. The curve shows a remarkably good agreement to the experimental curve of Fig. 6, with the oscillatory fall in response at high frequencies taking a very similar form. Under closer examination, it is found that there is a phase shift as well as sharper reduction in amplitude in the oscillations in the experimental curve, although the overall form and frequency of the oscillations is similar. The discrepancies in both the phase and amplitude of the oscillations are probably caused by neglecting both the effect of the stray inductance in the output connections to the transformer and the frequency dependance of permeability and loss of the ferrite cores, used to build the transformer, in the model. Examination of the voltage transfer function above reveals that the oscillations are caused by the increasingly bad mismatch, as the frequency is increased, between the output impedance of the transformer and the load due to the decreasing impedance presented by the parallel stray winding capacitance. This mismatch results in reflections, at the load, whose amplitude increases with frequency and leads to an apparent oscillatory modulation of the frequency response curve.

V. DISCUSSION

The performance of the transformer as a pulse transformer exceeds anything that could be achieved for any conventional magnetically cored device with similar voltage rating and gain or turns ratio that the authors are aware of. It is also clear from the modeling discussed that both the rise time performance and droop of this type of device could be fur-

ther enhanced. A reduction in the stray capacitance of the cable windings would improve its bandwidth and rise time and a further increase in inductance by increasing the number of cores or turns in the windings would improve the droop. Perhaps the most important aspect of this work is the frequency response characteristics of the transformer, which indicates that this type of transformer should be capable of development as a continuously excited power transformer whose bandwidth capabilities, particularly at high frequencies, will offer substantial improvements on the performance capabilities of conventional transformers wound on magnetic cores.

ACKNOWLEDGMENTS

This work was partly carried out with funding from the Naval Surface Warfare Center under the Prime Contract No. N60921-91-C-0078 managed by the Space Power Institute at Auburn University, AL. The authors gratefully acknowledge the assistance of G. Branch in checking both the manuscript and the calculations.

[1] J. O. Rossi and P. W. Smith (unpublished).
[2] P. N. Graneau, J. O. Rossi, and P. W. Smith (unpublished).
[3] J. Millman and H. Taub, in *Pulse, Digital, and Switching Waveforms* (McGraw Hill, New York, 1985), Chap. 3.
[4] M. Akemoto and S. Takeda, Proceedings of the 9th International Pulsed Power Conference, 1993 (unpublished), p. 316.
[5] *Philips Components Technical Handbook*, Book 3, Part 2a (Philips Components, London).
[6] *Handbook of Wiring, Cabling and Interconnecting for Electronics*, edited by C. A. Harper (McGraw-Hill, New York).
[7] The British Standards Institution, BS2316 specification for URM 67 cable.
[8] C. A. Pirrie, P. N. D. Maggs, and P. W. Smith, Proceedings of the 8th IEEE International Pulsed Power Conference, San Diego, 1991 (unpublished), p. 310.
[9] E. C. Snelling, in *Soft Ferrites, Properties and Applications* (Butterworth, New York, 1988), Chap. 7.
[10] R. A. Chipman, in *Transmission Lines* (McGraw-Hill, New York, 1968), Chap. 7.
[11] T. Dreher, Electron. Eng. **X**, 71 (1969).
[12] *Matlab* (MathWorks, Prentice-Hall, New York, 1992).